SYNCHROINFO JOURNAL

www.media-publisher.eu/synchroinfo-journal

EMC IMPLICATIONS OF FREQUENCY-DEPENDENT GROUNDING IMPEDANCE IN INDUSTRIAL AUTOMATION EQUIPMENT

Valeriy V. Polyanov [1], **Sergey V. Toropov** [2]

[1] Siberian Transport University, Novosibirsk, Russia;

[2] OJSC Russian Railways, Novosibirsk regional communications center, Novosibirsk, Russia;

polyanovvv@mail.ru, toropovs@wsr.ru

ABSTRACT

This paper presents a quantitative model of induced voltage in power supply cables of industrial equipment, focusing on the shielding effectiveness provided by the cable screen (PE conductor) as a function of its grounding resistance and the frequency of the disturbing magnetic field in the range up to 10 kHz. Based on a quasi-stationary three-conductor approximation with dominant inductive coupling, the analytical expression reveals a sharp threshold behavior: induced voltage magnitude remains low only at very small grounding resistances (1-4 Ω at power frequency). At audio and higher frequencies (0.8-10 kHz), shielding efficiency degrades markedly due to the growing inductive reactance of the “screen-ground” drainage path, rendering compensation ineffective even at resistances still considered acceptable under some 50 Hz norms (up to 30 Ω). Numerical results for grounding resistances spanning 0.1 Ω to 100 MΩ and selected frequencies explain several persistent field observations: seasonal surges in failures of CNC electronics and control modules during periods of elevated soil resistivity (drought, freezing), damage to microcontrollers, power switches, and input circuits despite conventional overcurrent protection, and limited success of localized mitigation when long parallel cable routes act as open inductive loops. The study emphasizes that grounding impedance must be regarded as strongly frequency-dependent. Reliable electromagnetic immunity in industrial environments, where soil resistivity often ranges from 500 to 5000 Ω·m or higher, requires low-impedance designs across the relevant spectrum: extended electrode configurations (multiple rods, grids, deep wells), ground enhancement materials, rational cable routing, consistent shielded cabling, staged surge protection with minimized inductance, and, where practical, fiber-optic interfaces. In multilayered soils typical of industrial sites, accurate high-frequency prediction necessitates Wenner/Schlumberger measurements followed by layered inversion modeling. The findings advocate a systemic approach to EMC rather than isolated fixes. Future investigations will target optimized grounding topologies for high-resistivity soils, inclusion of distributed parameters at tens of kHz, detailed multilayer simulations, and field verification.

DOI: 10.36724/2664-066X-2025-11-6-2-11

Received: 10.09.2025

Accepted: 28.11.2025

Citation: Valeriy V. Polyanov, Sergey V. Toropov, "EMC Implications of Frequency-Dependent Grounding Impedance in Industrial Automation Equipment", *Synchroinfo Journal* **2025**, vol. 11, no. 6, pp. 2-11.

Licensee IRIS, Vienna, Austria.

KEYWORDS: *electromagnetic compatibility, EMC, grounding, induced voltage, CNC, machine tool industry, industrial equipment, industrial automation.*

1 Introduction

The integration of digital technologies into manufacturing significantly increases the dependence of computer numerical control (CNC) machines and other automated systems on the electromagnetic immunity of their electronic components. Field measurements and laboratory tests [1, 2] indicate that a substantial proportion of electronic equipment failures in industrial environments result from impulsive overvoltages as well as deficiencies in grounding and equipotential bonding systems. According to various sources, such failures may account for up to 60 % of all incidents related to power quality and electromagnetic compatibility (EMC) [3, 4]. The main pathways for the penetration of induced voltages into power supply cable lines of industrial equipment are illustrated in Figure 1.

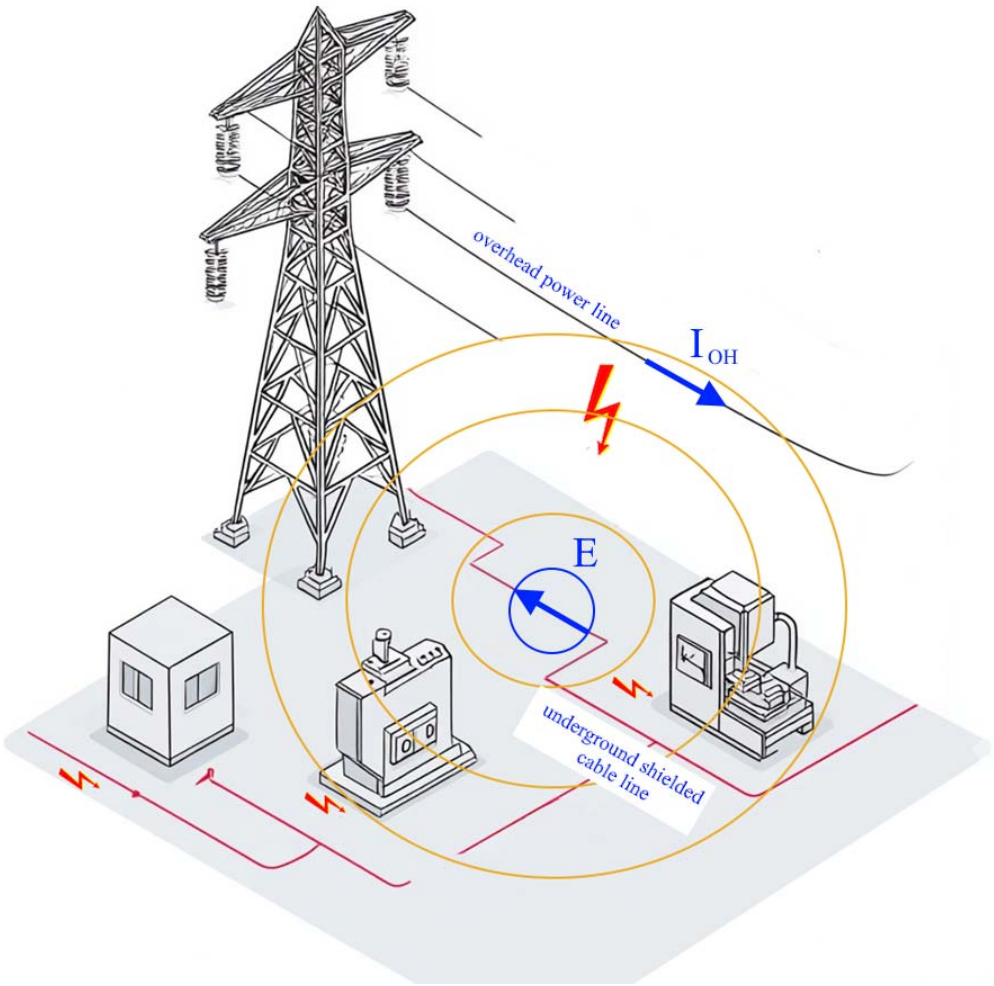

Figure 1. Penetration of extraneous voltages into the power supply cable line

The siting of production facilities in industrial areas necessitates consideration of several key factors. First, equipment, including CNC systems, electronics, longitudinal automation lines, and power supply networks, is exposed to intense electromagnetic fields generated by high-voltage transmission lines and traction power systems. Second, the upper soil layers near the facilities often exhibit high specific resistivity, which complicates the design and construction of effective grounding systems.

Precisely under such conditions, traditional grounding approaches, such as standard vertical electrodes 3-6 m in length, horizontal strips, and similar configurations, frequently prove either ineffective or economically unjustifiable. This highlights the pressing need to develop optimal solutions that are both technically efficient and resource-saving [5].

Modern design of industrial facilities demands a comprehensive consideration not only of primary energy supply technologies but also of a thorough elaboration of all auxiliary engineering systems, including grounding and lightning protection arrangements. As emphasized in study [6], the effectiveness of design solutions directly depends on the quality of geotechnical investigations, the correctness of the selected grounding scheme, the reliability of soil property assessments, and strict adherence to applicable normative requirements.

Modern practice demonstrates that analyzing electromagnetic disturbances solely at the fundamental frequency of 50 Hz is insufficient. In actual operating conditions of power systems and traction networks, a significant portion of the energy is concentrated in the kilohertz range due to harmonics, switching transients, magnetization inrush currents, fault conditions, and fast transients that are not adequately limited by conventional overcurrent protective devices [2, 3].

In [6], it is shown that classical methods fail to account for the spectral characteristics of influencing lines; accordingly, a mathematical model for railway infrastructure in phase coordinates was proposed, based on a system of differential equations solved in the Laplace domain.

The issue of electromagnetic influences extends beyond cable lines alone. Digital models have been developed for the electromagnetic effects of multi-wire traction networks (25 kV) and overhead power lines on parallel pipelines, taking into account actual train movement profiles, phase current distributions, and distributed pipeline grounding [7]. It was found that under typical operating conditions, maximum induced voltages reach 300-700V far exceeding the 60V safety limit, while in fault scenarios on 220 kV lines (single-phase short circuits), voltages can rise to several kilovolts at structure extremities.

In paper [8], the authors examine practical aspects of transitioning from electromechanical relays to microprocessor-based relay protection and automation devices (MPRPD) at substations. MPRPDs are considerably more susceptible to transient and high-frequency disturbances (lightning strikes, switching overvoltages, single-phase-to-ground faults), which, in the absence of adequate EMC measures, lead to malfunctions, false tripping, and commissioning delays. Emphasis is placed on grounding architecture (separation of power and secondary grounding loops, shielding, foundation grids) and the limitations of retrofitting legacy substations.

The theoretical basis for inductive coupling calculations rests on models that include earth-return currents, multi-conductor equivalent circuits, and geometry- and soil-dependent mutual inductances [9, 10]. A decisive factor is the frequency-dependent impedance of disturbance current paths in the grounding system: at 50 Hz, resistive spreading dominates, but in the range up to 10 kHz, the inductance of PE conductors prevails, causing a sharp rise in residual overvoltages at equipment inputs [11, 12]. Therefore, core EMC, measures shielding, cable routing, and grounding, must be analyzed with respect to the actual spectral content of electromagnetic fields, taking into account parallel route length and separation, the mutual inductance matrix, and line parameters [13, 14].

Spectral analysis of currents and voltages in power and traction networks shows considerable electromagnetic energy in the band up to 10 kHz during switching operations, fault disconnections, and high-power converter activity [1-3]. Even when regulatory clearance zones around power facilities are respected, long power and signal cables inevitably create conductive loops and common-mode paths that remain continuously exposed to electromagnetic fields. Minimum horizontal separation distances from overhead line conductors provide electrical safety and operational reliability but do not prevent inductive coupling into extended metallic structures and cables located beyond these zones [15]. In such conditions, the primary controllable parameter for electromagnetic immunity is the frequency-dependent impedance of the grounding and equipotential bonding system, which ultimately determines disturbance currents and voltages at the inputs of sensitive modules during common-mode events [18].

The objective of the present study is to quantitatively characterize the dependence of induced voltage in a power line on the grounding resistance of the cable screen (PE conductor) and the frequency of the disturbing source in the range of 50 Hz to 10 kHz, thereby substantiating practical recommendations for the operation of CNC machines and automated industrial equipment.

2 Methods

The model is based on a quasi-stationary three-conductor equivalent circuit shown in Figure 2. Within this framework, the electromagnetic influence of an overhead power line (OHL) on the core (C) of an underground shielded cable line is considered over a section of length l. The influencing line represents the nearest power feeder or a parallel cable line. The shield (S) corresponds to the metallic sheath of the cable with equivalent impedance Z_s, grounded at both ends of the section. In the present study, the affected line is taken as the phase conductor supplying power to an electronic module, referenced to ground (earth) as the return path.

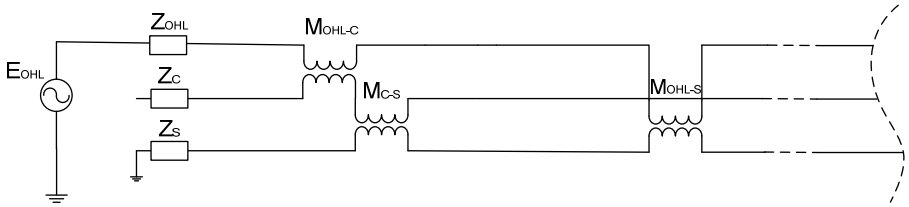

Fig. 2. Equivalent circuit of a single-conductor shielded line under magnetic influence

The mathematical description of the propagation of currents and voltages induced by magnetic coupling in each conductor is provided by a system of differential equations, the order of which depends on the number of conductors forming the unified electromagnetic system. For the power supply cable line under consideration consisting of the core and the shield the system comprises four equations:

$$\begin{cases} \cdot \frac{dU_C}{dx} = (R_C \quad _C) \cdot I_C \quad M_{C-S} \quad M_{C-OHL} \cdot \ _{OHL} \cdot \ ^{-\gamma x}, \\ -\frac{dI_C}{dx} = (G_C \quad C_C) \cdot U_C + (G_{C-S} \quad C_{C-S}) U \ _C \ U \ _S, \\ -\frac{dU_S}{dx} = \left(R_S \ R \ _{ground} \quad _S \cdot \ I_S \quad M_{C-S} \quad M_{S-OHL} \cdot \ _{OHL} \cdot \ ^{-\gamma x}, \right. \\ -\frac{dI_S}{dx} = (G_S \quad C_S) \cdot U_S + (G_{C-S} \quad C_{C-S})(U_S \ U \ _C). \end{cases} \quad (1)$$

where R_k, L_k, G_k, C_k are the self-parameters of the k-th conductor;

$M_{i\text{-}k}$, $G_{i\text{-}k}$, $C_{i\text{-}k}$ are the mutual parameters between the i-th and k-th conductors, computed across the frequency spectrum;

U_k, I_k are the voltages and currents in the respective conductors.

Equation system (1) enables a rigorous derivation of the induced voltage on the core as a function of the frequency of the external electromagnetic field and the shield grounding resistance. Since inductive coupling dominates in the low-frequency range of 50 Hz to 10 kHz, capacitive coupling and distributed effects are neglected. Thus, the magnitude of the core EMF can be expressed as:

$$E_C = j\omega I_{OHL}(M_{OHL\text{-}C}) - j\omega I_S(M_{C\text{-}S}) \quad (2)$$

The shield current is governed by the loop equation:

$$j\omega I_{OHL}(M_{OHL\text{-}S}) = I_S(R_S + R_{ground} + j\omega L_S) \quad (3)$$

Consequently, the induced voltage on the core as a function of frequency and grounding resistance takes the form:

$$E_C(\omega, R_{ground}) = j\omega I_{OHL}(M_{OHL\text{-}C}) - j\omega(M_{S\text{-}C}) \cdot j\omega I_{OHL}(M_{OHL\text{-}S})/(R_S + R_{ground} + j\omega L_S) \quad (4)$$

The grounding resistance of a single vertical electrode, accounting for the climatic seasonality coefficient of soil resistance, is determined by the following expression [17]:

$$R_{ground} \ k \ _1 \frac{\rho}{2\pi L} \ln \ \frac{2L}{d} \ 0 \ \ ,5 \ln \frac{4t+L}{4t-L}), \quad (5)$$

where k_1 is the frost penetration coefficient, which accounts for seasonal variations in soil temperature; L is the electrode length, m; ρ is the soil resistivity, Ω·m; t is the depth from the ground surface to the midpoint of the electrode, m; d is the electrode diameter, m.

The selection of electrode parameters is performed to ensure compliance with the normative grounding resistance values as required by applicable standards [18], while also considering the geological structure of the soil, the density of infrastructure in the installation area, and techno-economic criteria.

In industrial zones, soil resistivity is the decisive factor in determining the type, configuration, and dimensions of grounding systems, as it directly governs the current spreading resistance and the surface potential gradient. Under typical industrial site conditions (factories, substations, CNC-equipped workshops, and power-intensive facilities), soil resistivity values vary over a wide range: from 10-150 Ω·m in marshy and moist loamy soils to 1000-5000 Ω·m (and occasionally up to 40 kΩ·m) in dry sandy, rocky, stony, or made-ground areas commonly found on industrial premises. High soil resistivity significantly impairs the dissipation of short-circuit currents, impulsive overvoltages, and lightning discharges, resulting in elevated ground potential rise and increased step and touch voltages. Seasonal fluctuations in ρ necessitate a conservative design approach: calculations must be based on worst-case conditions, supplemented by regular periodic monitoring of grounding resistance.

Thus, accurate determination of soil resistivity during the geotechnical survey stage not only ensures compliance with electrical safety requirements but also enables optimization of material costs by avoiding both underestimation of risks (unsafe conditions) and overdesign (excessive expenditure) of the grounding system.

3 Results

Due to range of soil resistivity the grounding resistance R_{ground} was varied numerically from 0.1 Ω to 100 MΩ, covering operational conditions from normative-compliant grounding devices to degraded or faulted states. Figure 3 presents the calculated dependence of the grounding resistance R_{ground} on soil resistivity ρ for a single vertical electrode of length 3m and diameter 16 mm.

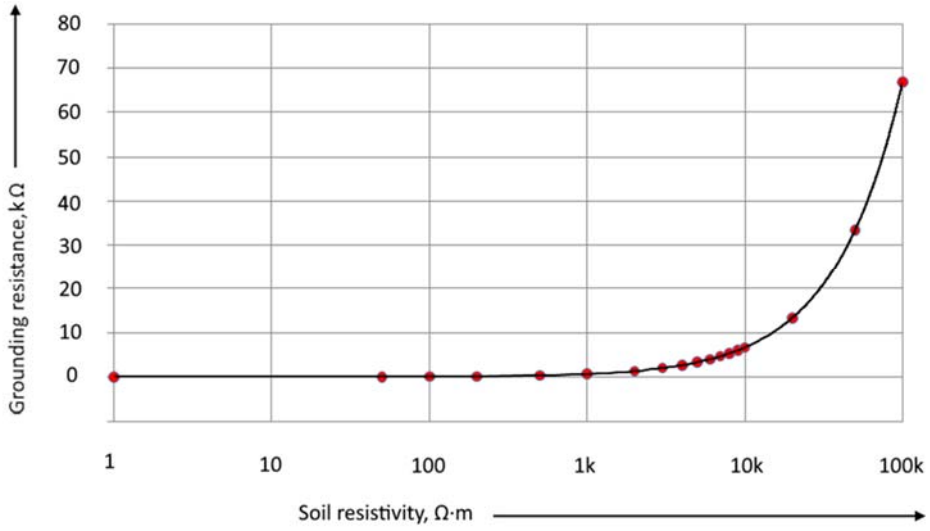

Fig. 3. Grounding resistance R ground on soil resistivity ρ

External disturbances were interpreted using standardized test models from the IEC 61000 series, which provide representative spectral energy distributions up to 10 kHz for industrial environments, as well as industry-specific guidelines for protection of communication lines near traction networks, indicating significant induced voltages on parallel conductors tens of meters from the source [16]. Practical separation distances from influencing overhead lines were referenced to the clearance zone norms for electric

power facilities [11]. EMC requirements were considered in the context of core industrial immunity standards, surge protective device coordination, and grounding system architectures [16].

The numerical parameters used in the modeling are presented in Table 1. The values are normalized to the orders of magnitude typical for real extended parallel routings in order to reveal threshold effects.

Table 1

Parameters for numerical modeling

Parameter	Value
Mutual inductance M_{OHL-C} (influencing line – core)	3 mH
Mutual inductance M_{OHL-S} (influencing line – shield)	4 mH
Mutual inductance M_{S-C} (shield – core)	30 mH
Inductance of the shield loop L_S	33 mH
Shield resistance R_S	3.4 Ω

The computation results are presented in Fig. 4. For an influencing line current magnitude of $|I_{OHL}|$ = 1 A at 50 Hz, the induced voltage magnitude on the core $|U_C|$ as a function of grounding resistance R_{ground} increases monotonically, showing a distinct inflection point when transitioning from the region of low resistances to moderate values. At grounding resistances on the order of 0.1-1 Ω, the shield current is high, and its phase is close to providing nearly quadrature compensation of the induced EMF. At R_{ground} up to 4 Ω, a noticeable increase in $|U_C|$ becomes apparent, followed by a steep section of the curve in the 4-30 Ω interval, after which the shielding effectiveness drops sharply. In the grounding resistance range of 30 Ω to 100 MΩ, the shielding effect is negligible.

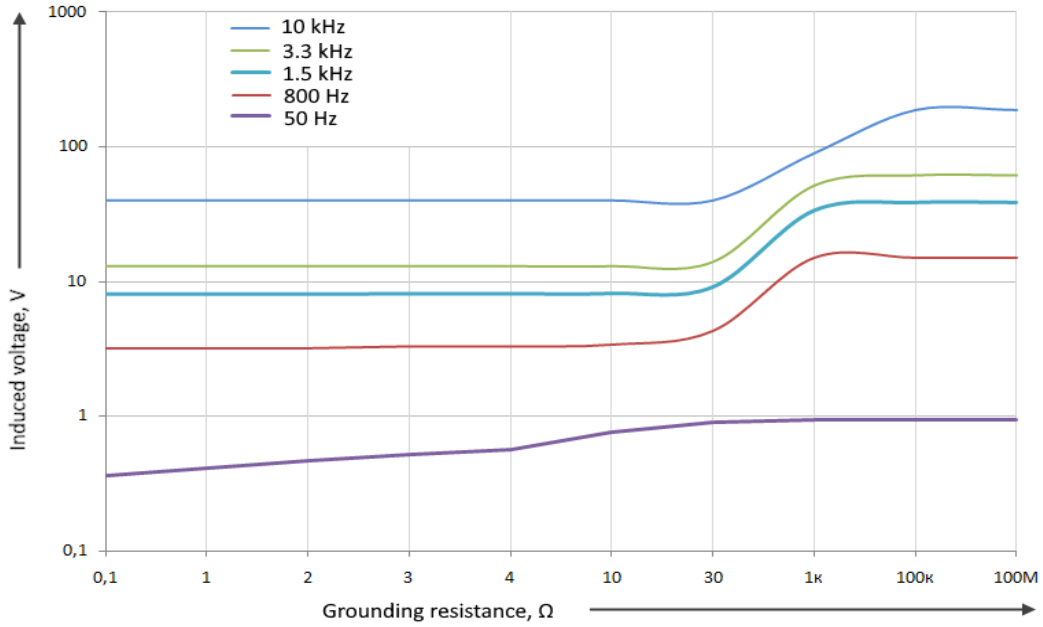

Fig. 4. Calculated dependence of the induced voltage on grounding resistance across the frequency spectrum

In the audio-frequency band (0.8–3.3 kHz), the highest shielding effectiveness is achieved at grounding resistances up to 30 Ω, whereas at resistances above 1 kΩ the shielding effect is virtually absent. As the frequency of the influencing current rises, the protective performance of the shield further deteriorates. For example, at 10 kHz, an avalanche-like increase in induced voltage is observed up to grounding resistance values as high as 100 kΩ, indicating an emergency (fault) operating condition of the grounding system (given the normative requirements of 2 to 30 Ω [11]).

To evaluate the feasibility of achieving the required grounding resistance for effective shielding (not exceeding 30 Ω), fig. 5 presents the calculated dependence of the grounding resistance of a single vertical electrode on its length (midpoint burial depth t = L/2, climatic coefficient k_1 = 1 (reference non-frozen condition) and soil resistance is 500 Ω.

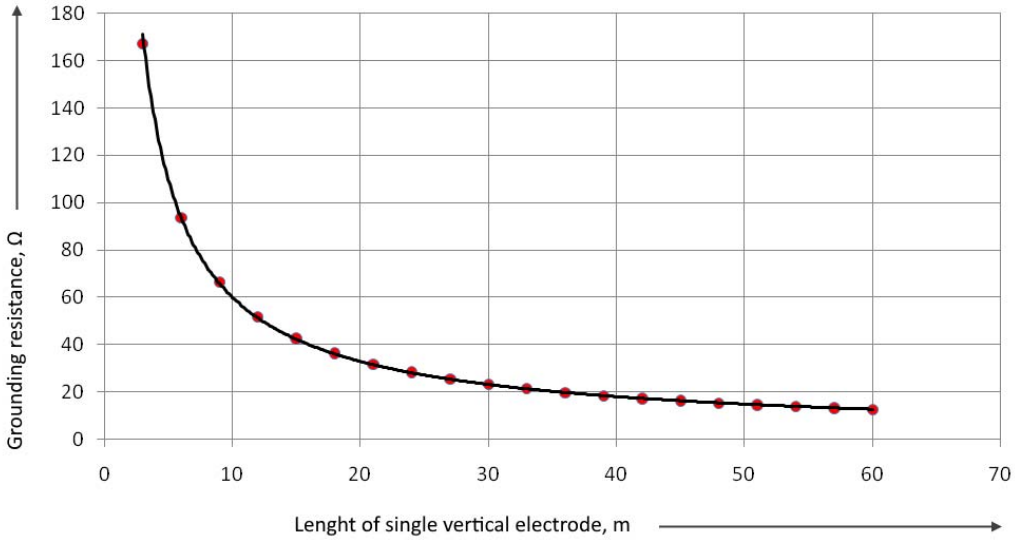

Fig. 5. Grounding resistance on the length of a single vertical electrode

The results demonstrate that, under such soil conditions, even a relatively long single electrode (L = 10 m) yields R ≈ 60 Ω, while L = 20 m still gives ≈ 35 Ω. Achieving R ≤ 30 Ω would require an impractically long rod well over 25 m in most realistic scenarios.

4 Discussion

Equation (4) reflects the presence of two opposing mechanisms: the primary induced EMF in the core increases proportionally to ω, whereas the compensating contribution from the shield is proportional to ω² in the numerator but is limited by the frequency-dependent denominator. As frequency rises, the inductive component jωLэ increases the impedance of the "shield–ground" loop, thereby reducing the shield current. Consideration of capacitive couplings and distributed effects at the upper boundary of the frequency band (10 kHz) is deliberately omitted here and may be addressed in future studies, since in practical switching regimes of power systems and traction networks the dominant contribution to the induced EMF in the configuration under study comes from inductive coupling [6].

In multilayered soils, which are typical for industrial sites, the interpretation of Wenner and Schlumberger measurements is essential, involving the construction of a layered soil model to accurately predict the behavior of the grounding system in the kilohertz frequency range, where inductive effects further degrade performance. This layered modeling approach is necessary because apparent resistivity data from Wenner (equal probe spacing) or Schlumberger (variable current electrode separation) arrays reveal vertical variations in soil structure when plotted against probe spacing. At frequencies from several hundred Hz to tens of kHz, relevant to switching transients, harmonics, and high-frequency disturbances in power and traction systems, the inductive reactance of grounding conductors and paths becomes dominant. In multilayer soils, high-resistivity upper layers increase the effective impedance of current drainage paths, while deeper low-resistivity strata may not be fully utilized due to current confinement. Accurate layered models enable reliable prediction of frequency-dependent grounding impedance, step/touch voltages, and electromagnetic immunity of connected equipment, preventing underestimation of risks in transient conditions.

The dependence of grounding resistance on the length of electrode (Fig. 5) underscores that in industrial zones with moderate to high soil resistivity, relying on a single vertical electrode is generally insufficient to meet stringent low-impedance requirements (≤ 30 Ω) needed for reliable high-frequency compensation of induced voltages in shielded power cables. Therefore, practical implementations typically necessitate multiple parallel rods, extended horizontal conductors or grids, deep wells reaching lower-resistivity layers, or the application of conductive backfill materials. Future research will focus on investigating the optimal configuration of grounding electrodes (earthing arrangements) for soils characterized by low electrical conductivity (high resistivity, typically ρ > 0.5-40 kΩ·m), which are common in many industrial zones with dry sandy, rocky, made-ground, or seasonally frozen substrates.

The obtained dependencies provide a clear explanation for effects that are consistently observed in real-world operation. First, a distinct threshold in grounding resistance R_{ground} of approximately 4-10 Ω has been identified, beyond which even a minor increase in spreading resistance and/or deterioration of metallic bonding leads to an avalanche-like rise in induced voltage to hazardous levels. This finding correlates with the well-documented seasonal increase in CNC electronics failures during periods of drought and freezing, when soil resistivity and transition resistances of jumpers rise significantly, despite formally compliant values measured at 50 Hz [13]. Second, the frequency dependence elucidates why conventional overcurrent protective devices fail to prevent damage to microcontrollers, power switches, and input circuits: circuit breakers and fuses do not limit the amplitude or rate of rise of fast overvoltages and transient processes. The resulting engineering implication is the necessity to implement staged surge protective devices with minimal connection lengths and low-inductance discharge paths to the PE busbar, thereby reducing the $|j\omega L|$ term in the kilohertz range [15]. Third, even when clearance zones around outdoor switchgear and overhead lines, as well as minimum distances from catenary systems, are observed, long power and signal cable routes connected to equipment remain exposed to electromagnetic induction as open inductive loops. In such cases, rational cable routing, additional shielding, transition to fiber-optic interfaces for control signals, and galvanic isolation enable a reduction in loop area and, consequently, in the primary induced EMF [19, 20].

Comparison of the present results with industry-specific guidelines for the protection of communication lines near railway catenary systems confirms that significant induced voltages can occur at distances of tens of meters from the source. In industrial shop-floor conditions, this corresponds to parallel power supply routes and cable trays running alongside main power feeders and transformers. This explains why localized mitigation measures applied only at the switchboard or machine level prove insufficient without a comprehensive solution encompassing the entire cable route and grounding system architecture.

5 Conclusion

This study developed a quantitative model describing the induced voltage in power supply lines of industrial equipment as a function of cable screen (PE conductor) grounding resistance and the frequency of the disturbing source in the 50 Hz – 10 kHz range. The derived analytical expression, based on a quasi-stationary three-conductor model with dominant inductive coupling, clearly reveals a pronounced threshold behavior: a sharp (avalanche-like) rise in induced voltage magnitude occurs when grounding resistance exceeds the narrow interval. Beyond this critical range the curve rapidly saturates, approaching the levels characteristic of an effectively ungrounded (open) screen condition.

These findings provide a physically consistent explanation for field phenomena: seasonal spikes in CNC electronics failures during dry summers and severe winters (when soil resistivity and contact resistances rise dramatically), systematic damage to input circuits, microcontrollers and power switches despite presence of conventional overcurrent protection, and insufficient performance of localized mitigation measures when long parallel cable routes remain exposed to power-frequency and harmonic magnetic fields.

The central practical implication is that grounding impedance must be treated as a strongly frequency-dependent parameter rather than a single 50 Hz value. Achieving and most importantly maintaining low impedance across the entire relevant spectrum becomes a key requirement for electromagnetic immunity of modern industrial automation.

In typical industrial site conditions, where soil resistivity frequently lies in the 500-40000 Ω·m range (and higher in made-ground or rocky areas), single vertical electrodes almost never suffice. Reliable performance demands extended configurations: multiple rods, horizontal conductors, meshed grids, deep wells reaching lower-resistivity strata, and/or application of ground enhancement materials (conductive backfill, bentonite mixtures).

The obtained results strongly support a systemic rather than local approach to EMC assurance: rational cable routing, consistent use of shielded lines, periodic verification of screen grounding quality, staged surge protection with minimized inductance, transition to fiber-optic interfaces where feasible, and, crucially, design of grounding and equipotential bonding systems with explicit consideration of the actual disturbance spectrum.

Future work will concentrate on optimization of grounding electrode configurations specifically for high-resistivity soils, incorporation of distributed line parameters at higher frequencies (tens of kHz), detailed numerical simulation of realistic multilayer profiles, and field validation on industrial test setups.

REFERENCES

[1] V. M. Avanesov, F. V. Yashchenko, A. Yu. Gaivoronsky, “Ensuring electromagnetic compatibility of secondary power supply sources,” *Sovremennye problemy fiziki, biofiziki i infokommunikatsionnykh tekhnologiy*. 2024. No. 14. URL: https://cyberleninka.ru/article/n/obespechenie-elektromagnitnoy-sovmestimosti-istochnikov-vtorichnogo-elektropitaniya (accessed: 12.12.2025).

[2] A. S. Podgorny, “Ensuring vehicle quality using an integrated electromagnetic environment monitoring system and prevention of electromagnetic compatibility conflicts,” *Izvestiya TulGU. Tekhnicheskie nauki*. 2024. No. 1. URL: https://cyberleninka.ru/article/n/obespechenie-kachestva-avtomobiley-s-ispolzovaniem-kompleksnoy-sistemy-monitoringa-elektromagnitnoy-obstanovki-i-preduprezhdeniya (accessed: 12.12.2025).

[3] L. A. Myasoedova, “Electromagnetic compatibility of power electrical network and electronic devices,” *Vestnik Amurskogo gosudarstvennogo universiteta. Seriya: Estestvennye i ekonomicheskie nauki*. 2023. No. 103. URL: https://cyberleninka.ru/article/n/elektromagnitnaya-sovmestimost-silovoy-elektricheskoy-seti-i-elektronnyh-ustroystv (accessed: 12.12.2025).

[4] H. W. Ott, “Electromagnetic Compatibility Engineering,” Hoboken: Wiley, 2009. 872 p. ISBN 978-0-470-18930-6.

[5] O. G. Evdokimova, “Development of methods and means to improve the efficiency of grounding devices in railway automation and telemechanics systems,” abstract of the dissertation for the degree of Candidate of Technical Sciences. St. Petersburg, 2013. 16 p.

[6] V. V. Polyanov, “Methodology for modeling electromagnetic compatibility on heavy-haul train sections,” Vestnik Uralskogo gosudarstvennogo universiteta putei soobshcheniya. 2016. No. 2(30). pp. 119–127. DOI 10.20291/2079-0392-2016-2-119-127.

[7] K. V. Suslov, A. V. Kryukov, P. V. Ilyushin, “Modeling electromagnetic influences of multi-wire traction networks on pipelines,” *Vestnik IrGTU*. 2023. No. 3. URL: https://cyberleninka.ru/article/n/modelirovanie-elektromagnitnyh-vliyaniy-mnogoprovodnyh-tyagovyh-setey-na-truboprovody (accessed: 12.12.2025).

[8] M. N. Movenko, B. S. Kompanets, “Influence of electromagnetic fields on the operation of relay protection and automation devices,” *Forum Molodykh Uchenykh*. 2025. No. 5(105). URL: https://cyberleninka.ru/article/n/vliyanie-elektromagnitnyh-poley-na-rabotu-ustroystvo-releynoy-zaschity-i-avtomatiki (accessed: 12.12.2025).

[9] V. V. Sapozhnikov, Vl. V. Sapozhnikov, V. I. Shamanov et al., “Reliability of railway automation, telemechanics and communication systems,” textbook. Moscow: Transport, 2002. 263 p.

[10] V. V. Polyanov, “Standardization of electromagnetic compatibility,” *Avtomatika, svyaz, informatika*. 2016. No. 7. pp. 18-21.

[11] “Rules for technical operation of consumer electrical installations,” Moscow: Prospekt, 2019. 280 p.

[12] V. V. Polyanov, S. A. Bessonko, “Methodology for calculating the error of linear structures diagnostic systems on heavy-haul train sections,” *Transport Aziatsko-Tikhookeanskogo Regiona*. 2023. No. 4(37). pp. 85-93.

[13] V. S. Verba, V. I. Merkulov, A. G. Teterukov, “Electromagnetic compatibility. Part 1. The role and place in on-board electronic complexes. Analysis of the problem status,” *Electromagnetic Waves and Electronic Systems*. 2025. pp. 5-19. DOI 10.18127/j5604128-202501-01.

[14] M. Pantelyat, P. Miasoedov, “Electromagnetic compatibility of technical objects and systems: a preliminary review of some software for computer modelling,” *Bulletin of NTU KhPI. Series: Problems of Electrical Machines and Apparatus Perfection. The Theory and Practice*. 2025. pp. 21-25. DOI 10.20998/2079-3944.2025.1.05.
[15] J. R. Carson, “Wave Propagation in Overhead Wires with Ground Return,” *Bell System Technical Journal*. 1926. Vol. 5. pp. 539-556.
[16] GOST 33398-2015, “Railway telecommunication. Protection regulation of lines communication against influence of a traction network of the electrified railways constant and alternating current,” 2015. Introduced 01.06.2016.
[17] A. A. Fedorov, G. V. Serbinovsky (eds.), “Handbook on Power Supply of Industrial Enterprises. In 2 books. Book 1. Design and Calculation Data,” Moscow: Energiya, 1973. 520 p.
[18] GOST 30331.1-2013 (IEC 60364-1:2005), “Low-voltage electrical installations. Part 1. Fundamental principles, assessment of general characteristics, definitions,” Moscow: Standartinform, 2014.
[19] V. Ďuriš, S. Chumarov, V. Ivanov, “Ensuring Electromagnetic Compatibility of Microprocessor Relay Protection Devices,” *TEM Journal.* 2025. pp. 1941–1947. DOI 10.18421/TEM143-03.
[20] R. Herrick, In. Chief, M. Akay et al., “Printed Circuit Board Design Techniques for EMC Compliance,” Series: IEC 62305: Protection against lightning. 2000.